Supporting Information for:

In-situ and Ex-situ Observations Assisted Understandings in the Effect of Ternary Strategy and Co-solvents for High-Efficiency Organic Solar Cells

Ruijie Ma[1,6], Cenqi Yan[2,6], Patrick Wai-Keung Fong[2], Jiangsheng Yu[2], Heng Liu[3], Junli Yin[1], Jianhua Huang,[5] Xinhui Lu[3], He Yan*[1,4], Gang Li[2]*

[1]Department of Chemistry, Guangdong-Hong Kong-Macao Joint Laboratory of Optoelectronic and Magnetic Functional Materials, Energy Institute and Hong Kong Branch of Chinese National Engineering Research Center for Tissue Restoration & Reconstruction, Hong Kong University of Science and Technology, Clear Water Bay, Kowloon, Hong Kong, China
Email: hyan@ust.hk
[2]Department of Electronic and Information Engineering, Research Institute for Smart Energy (RISE), The Hong Kong Polytechnic University, Hung Hom, Kowloon, Hong Kong, China
Email: gang.w.li@polyu.edu.hk
[3]Department of Physics, Chinese University of Hong Kong, Hong Kong, New Territories Hong Kong, China
[4]Institute of Polymer Optoelectronic Materials and Devices, State Key Laboratory of Luminescent Materials and Devices, South China University of Technology (SCUT), Guangzhou, 510640 China
[5]College of Materials Science and Engineering, Huaqiao University, Xiamen,361021, China
[6]R. Ma and C. Yan contribute equally to this work.

Characterization

UV-vis absorption spectra were measured using a Shimadzu UV-2500 recording spectrophotometer. Cyclic voltammetry (CV) measurements of targeted thin films were conducted on a CHI voltammetric analyzer in acetonitrile solution with 0.1 M tetrabutylammonium hexafluorophosphate (n-Bu4NPF6) as supporting electrolyte at room temperature by using a scan rate of 100 mV s-1 and conventional three-electrode configuration. AFM measurements were obtained by using a Dimension Icon AFM (Bruker) in a tapping mode. The grazing incidence X-ray scattering (GIWAXS) measurement was carried out with a Xeuss 2.0 SAXS/WAXS laboratory beamline using a Cu X-ray source (8.05 keV, 1.54 Å) and a Pilatus3R 300K detector. The incident angle was 0.2°. The samples for GIWAXS/GISAXS measurements were fabricated on silicon substrates using the same recipe for the devices. Contact angle tests were achieved by an Attension Theta Flex meter.

Solar cell fabrication and characterization

Solar cells were fabricated in a conventional device configuration of ITO/PEDOT:PSS/active layers/PFN-Br/Ag. The ITO substrates (~94% transmittance) were first scrubbed by detergent and then sonicated with deionized water, acetone and isopropanol subsequently, and dried overnight in an oven. The glass substrates were treated by UV-Ozone for 30 min before use. PEDOT:PSS (Heraeus Clevios P VP AI 4083) was spin-cast onto the ITO substrates at 4000 rpm for 30 s, and then dried at 150 °C for 15 min in air. The PM6:eC11:BN-T blends were dissolved in ortho-xylene (the donor concentration was 10.5 mg mL^{-1} for all blends), with 1-phenylnaphthalene (0.25% vol) as additive, and stirred on a 100 °C hotplate for 2 hours a nitrogen-filled glove box. The blend solution was spin-cast at 2300 rpm for 1:1.2:0, 2400 rpm 1:1.2:0.1, 2500 rpm for 1:1.2:0.2, for 50 s onto PEDOT:PSS films followed by a temperature anealing of 100°C for 5 min. The PM6:eC9:BN-T blends were dissolved in chlorobenzene (the donor concentration was 10.5 mg mL^{-1} for all blends), with 1,8-diiodooctane (0.7% vol) as additive, and stirred on a 100 °C hotplate for 2 hours a nitrogen-filled glove box. The blend solution was spin-cast at 3200 rpm for 1:1.2:0,

3400 rpm 1:1.2:0.1, 3600 rpm for 1:1.2:0.2, for 50 s onto PEDOT:PSS films followed by a temperature anealing of 100°C for 5 min. PFN-Br thin layers were coated on the active layer with 3000 rpm (0.5 mg mL^{-1}), followed by the deposition of Ag (90 nm) (evaporated under 1×10^{-3} Pa through a shadow mask). The optimal active layer thickness measured by a Bruker Dektak XT stylus profilometer was about 105 nm. The current density-voltage (J-V) curves of devices were measured using a Keysight B2901A Source Meter in glove box under AM 1.5G (100mW cm^{-2}) using a Enlitech solar simulator. The device contact area is 0.05 cm^2, device illuminated area during testing is 0.04 cm2, which is determined by mask. The EQE spectra were measured using a Solar Cell Spectral Response Measurement System QE-R3011 (Enlitech Co., Ltd.). The light intensity at each wavelength was calibrated using a standard monocrystalline Si photovoltaic cell.

SCLC Measurements

The electron and hole mobility were measured by using the method of space-charge limited current (SCLC) for electron-only devices with the structure of ITO/ZnO/active layer/PFN-Br/Ag and hole-only devices with the structure of ITO/PEDOT:PSS/active layers/MoO_x/Ag. The charge carrier mobility was determined by fitting the dark current to the model of a single carrier SCLC according to the equation: $J = 9\varepsilon_0\varepsilon_r\mu V^2/8d^3$, where J is the current density, d is the film thickness of the active layer, μ is the charge carrier mobility, ε_r is the relative dielectric constant of the transport medium, and ε_0 is the permittivity of free space. $V = V_{app} - V_{bi}$, where V_{app} is the applied voltage, V_{bi} is the offset voltage. The carrier mobility can be calculated from the slope of the $J^{1/2} \sim V$ curves.

Surface Tension Characterization

Contact angle measurements were carried out by an Attension Theta Flex meter, using water and ethylene glycol by sessile drop analysis. The surface tension values of films are calculated by the Wu method, in which:

$$\gamma_{Water}(cos\theta_{Water}+1)=\frac{4\gamma_{water}^{d}\cdot\gamma^{d}}{\gamma_{water}^{d}+\gamma^{d}}+\frac{4\gamma_{water}^{p}\cdot\gamma^{p}}{\gamma_{water}^{p}+\gamma^{p}}$$

$$\gamma_{EG}(cos\theta_{EG}+1)=\frac{4\gamma_{EG}^{d}\cdot\gamma^{d}}{\gamma_{EG}^{d}+\gamma^{d}}+\frac{4\gamma_{EG}^{p}\cdot\gamma^{p}}{\gamma_{EG}^{p}+\gamma^{p}}$$

$$\gamma=\gamma^{d}+\gamma^{p}$$

where θ is the contact angle of each thin film, and γ is the surface free energy of samples, which is equal to the sum of the dispersion (γ^{d}) and polarity (γ^{p}) components; γ_{water} and γ_{EG} are the surface tensions of the water and ethylene glycol; and γ_{water}^{d}, γ_{water}^{p}, γ_{EG}^{d} and γ_{EG}^{p} are the dispersion and polarity components of γ_{Water} and γ_{EG}.

Time-resolved UV-vis Experiments

The in-situ UV–vis spectra were measured using an F20 spectrometer (Filmetrics, Inc.). The light source was a halogen lamp with a spot size of 1.5 mm. An ITO/PEDOT:PSS-coated glass substrate was used as the reference so that the measured signal revealed the absorption/reflection of the organic thin film.

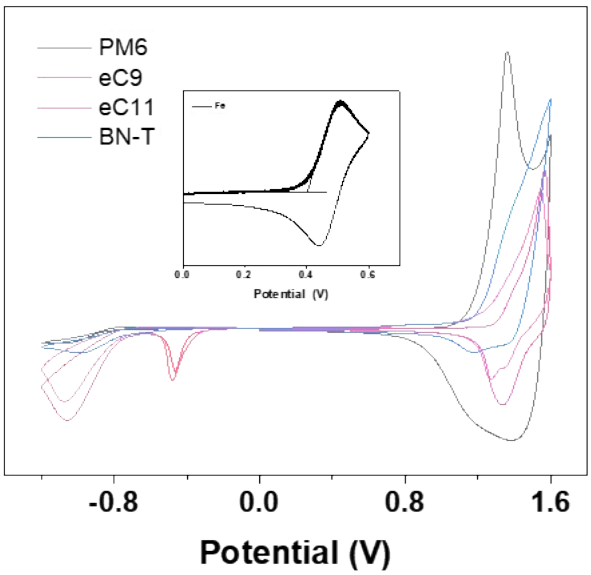

Figure S1. The CV curves of materials used and the reference.

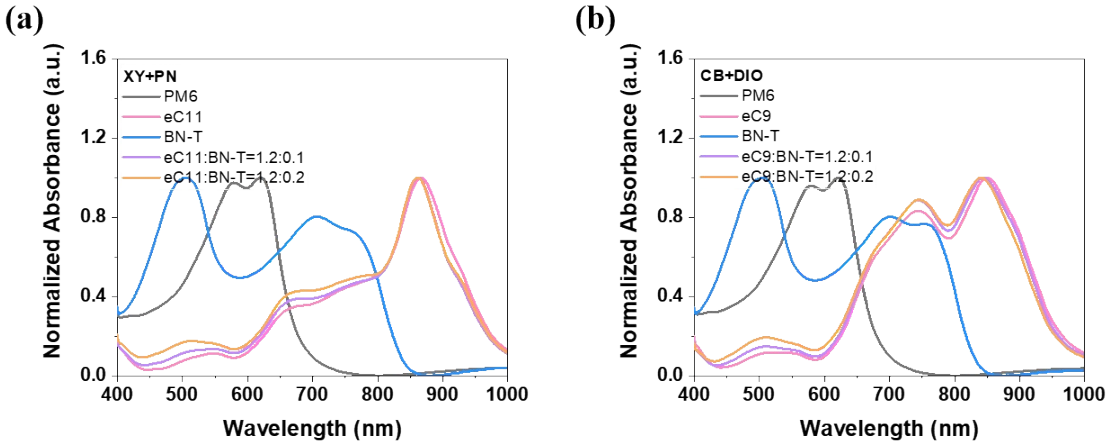

Figure S2. Film absorption spectra of (a) XY+PN and (b) CB+DIO processed pure donor and acceptor(s).

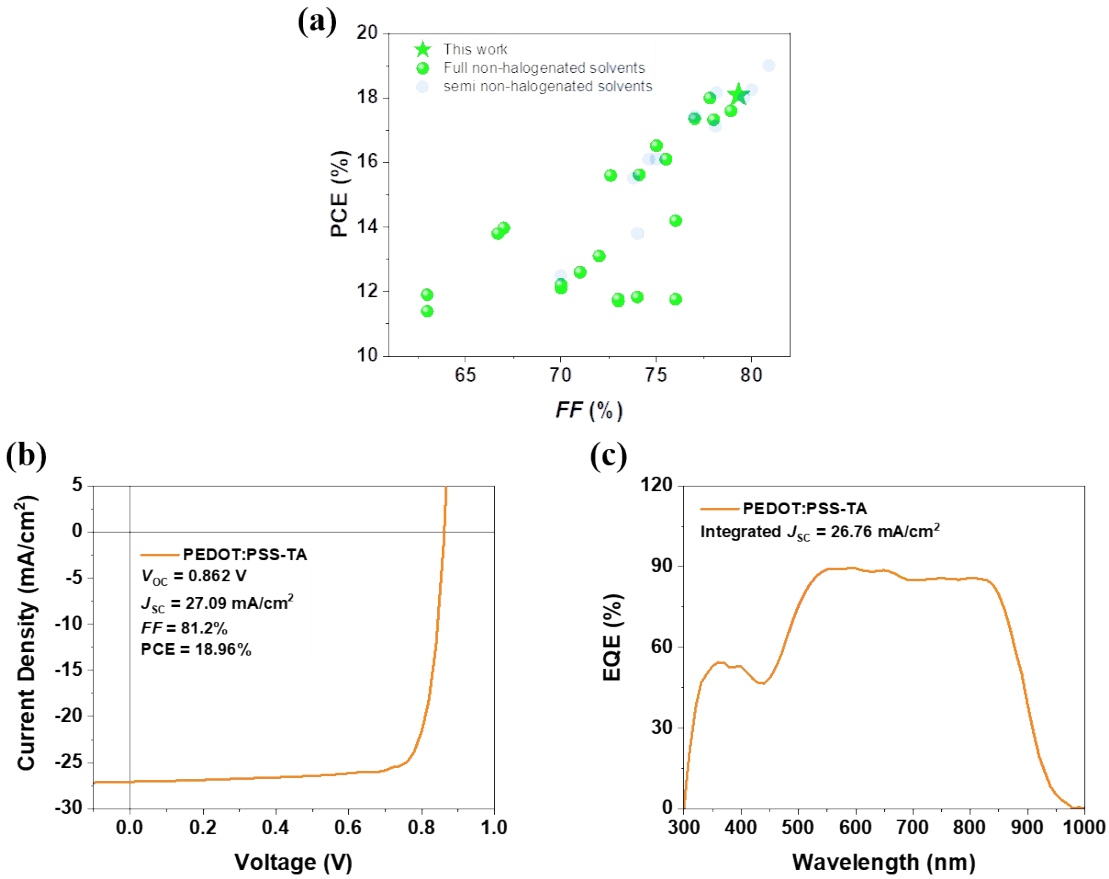

Figure 3. (a) Performance comparison of non-halogenated solvent(s) processed OSCs.

(b) *J-V* curve and (c) EQE spectrum of PEDOT:PSS-TA based devices.

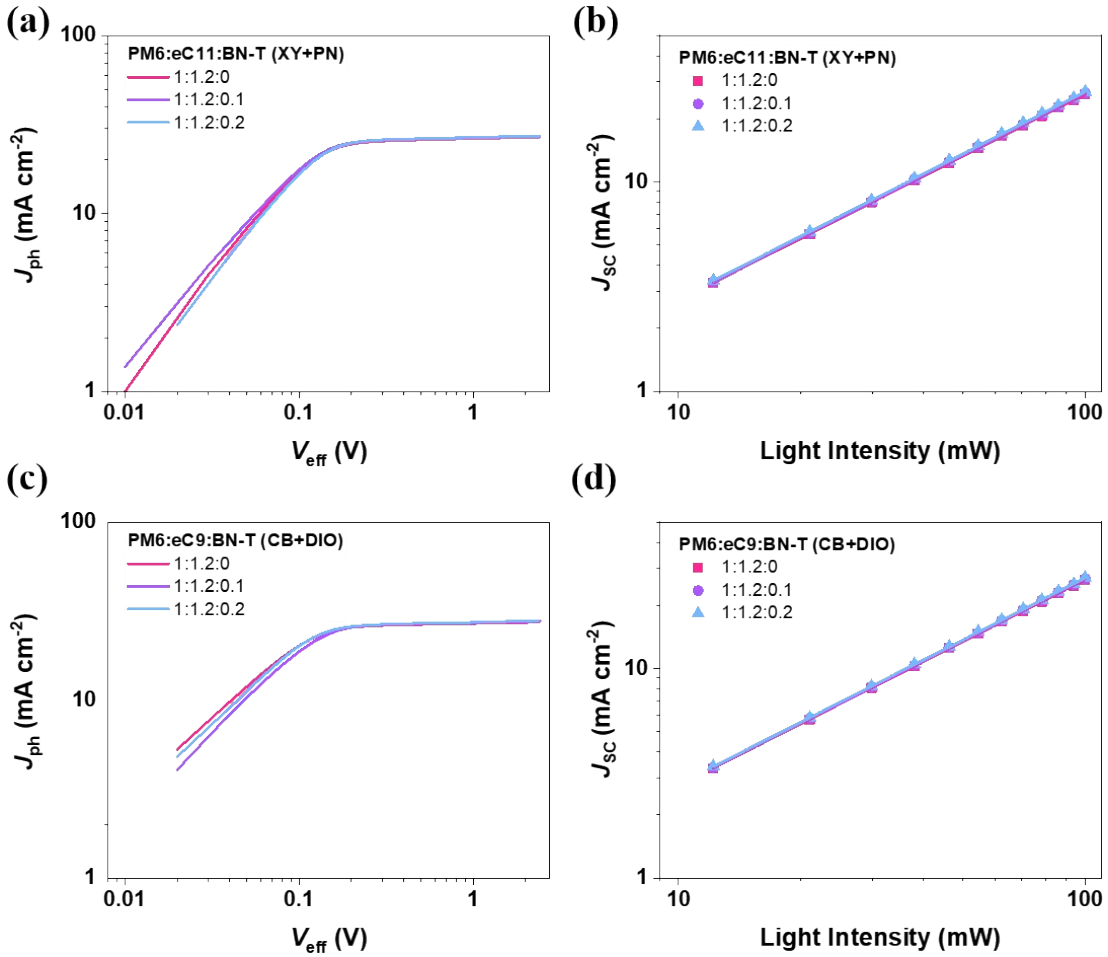

Figure S4. XY+PN processed PM6:eC11:BN-T composed OSCs' (a) J_{ph}-V_{eff} curves, (b) J_{SC} versus illumination intensity curves; CB+DIO processed PM6:eC9:BN-T-based OSCs' (c) J_{ph}-V_{eff} curves, (d) J_{SC} versus illumination intensity curves.

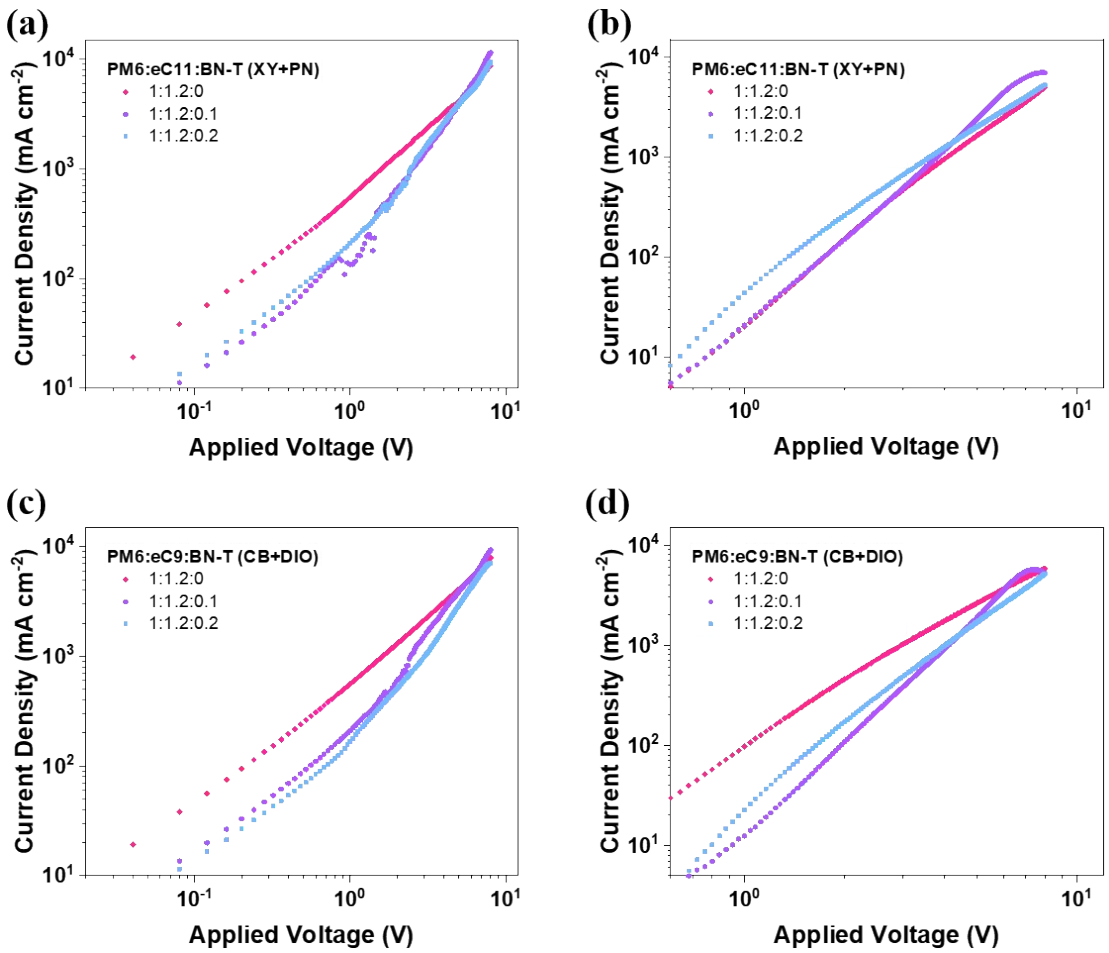

Figure S5. (a) Hole-only and (b) electron-only devices for PM6:eC11:BN-T (XY+PN); (c) hole-only and (d) electron-only devices for PM6:eC9:BN-T (CB+DIO)

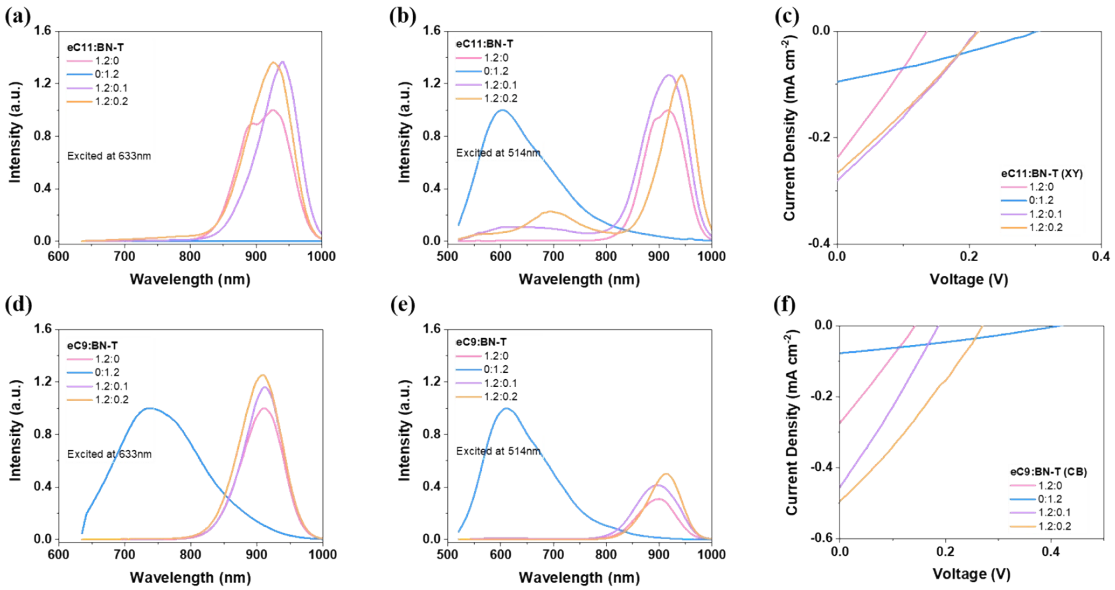

Figure S6. PL spectra of acceptors: (a) excited at 633 nm for eC11:BN-T (XY+PN), (b) excited at 514 nm for eC11:BN-T (XY+PN), (d) excited at 633 nm for eC9:BN-T (CB+DIO), (e) excited at 514 nm for eC9:BN-T (CB+DIO). Pure acceptor-based device results for (c) eC11:BN-T (XY+PN) and (f) eC9:BN-T (CB+DIO).

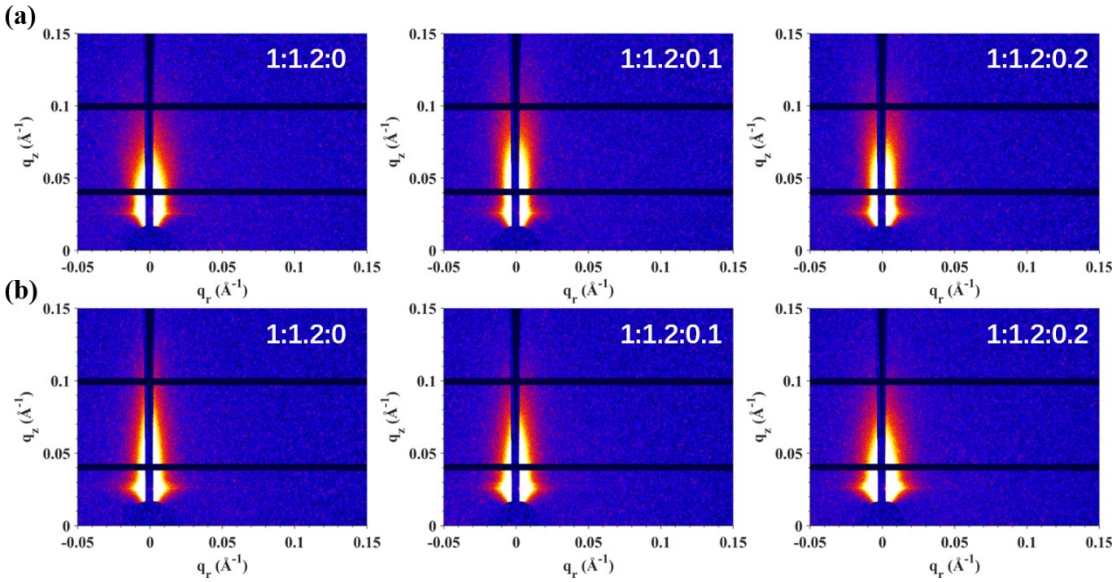

Figure S7. (a) PM6:eC11:BN-T (XY+PN) series films' 2D GISAXS patterns. (b) PM6:eC9:BN-T (CB+DIO) series films' 2D GISAXS patterns.

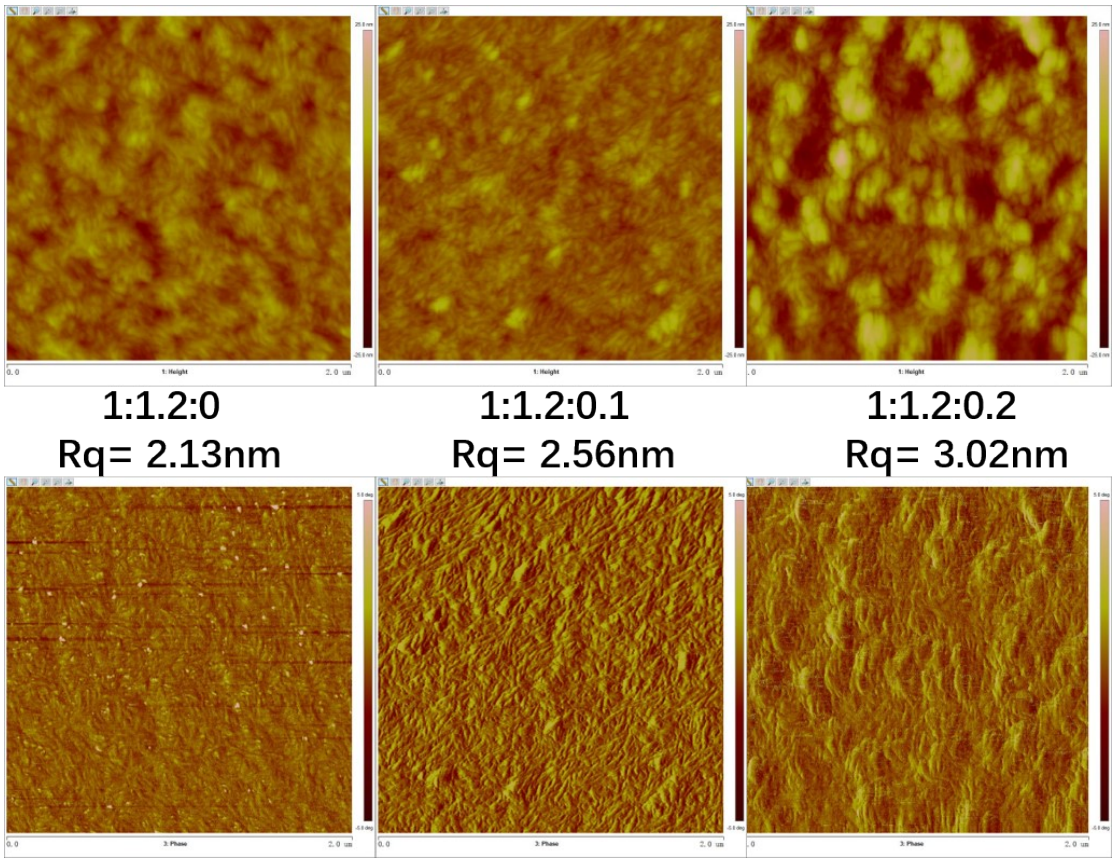

Figure S8. AFM height and phase images of PM6:eC11:BN-T (XY+PN).

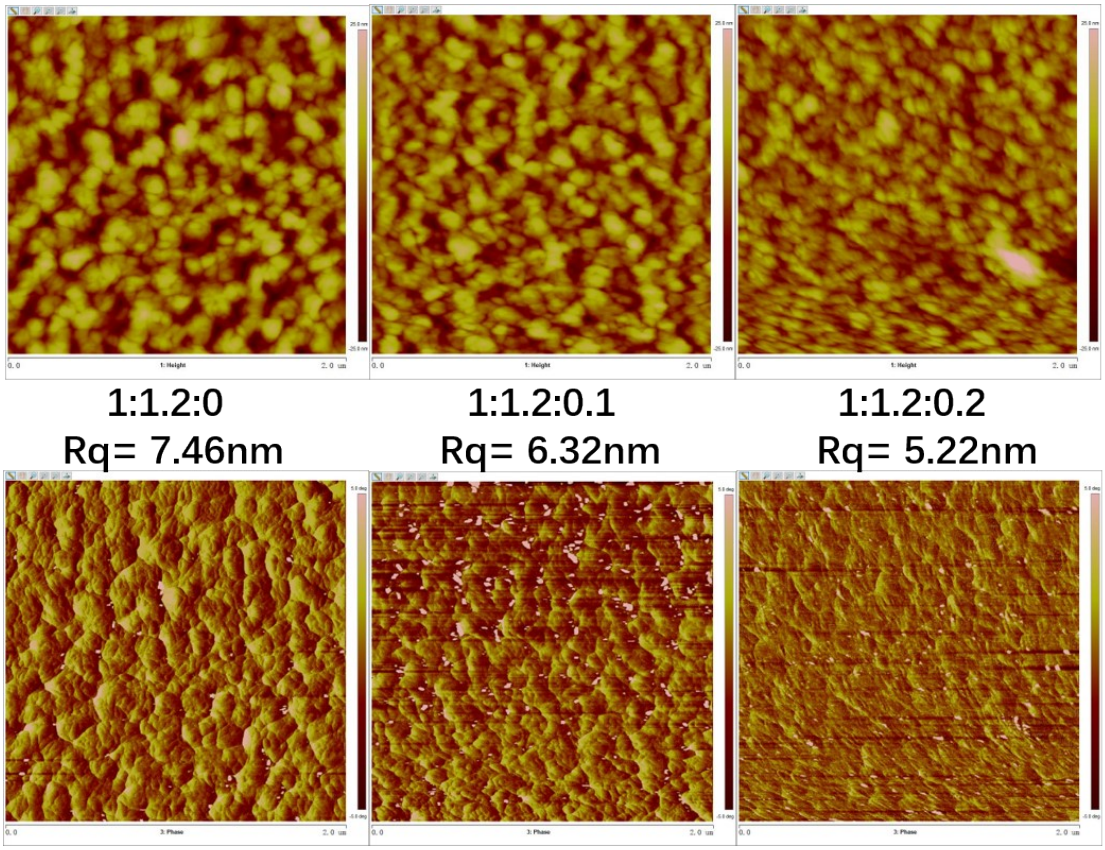

Figure S9. AFM height and phase images of PM6:eC9:BN-T (CB+DIO).

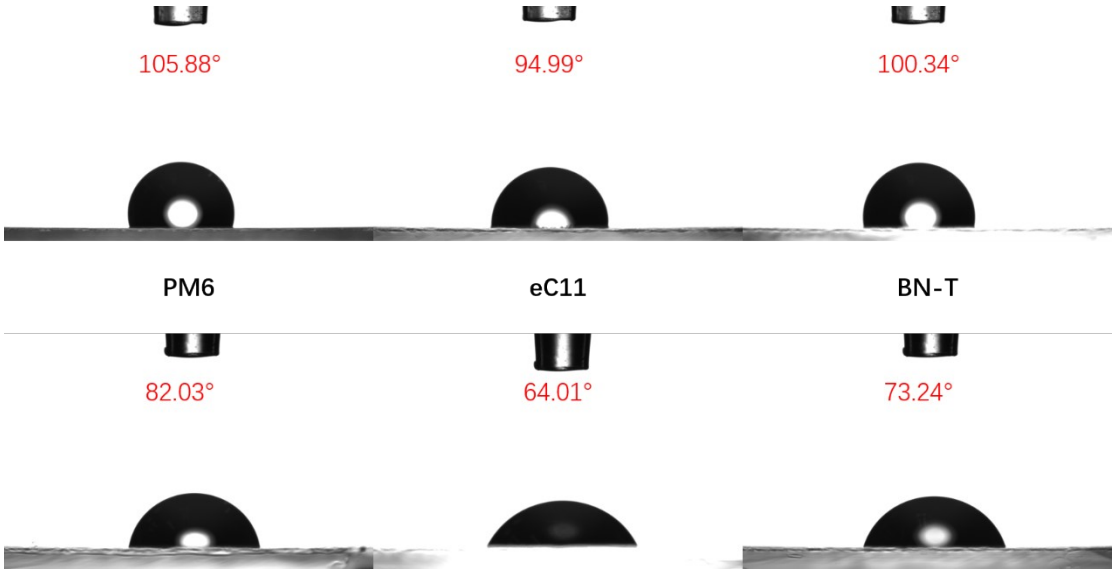

Figure S10. Contact angles of water (upper) and ethylene glycol (lower) on the films for PM6, BN-T, eC11 (XY+PN).

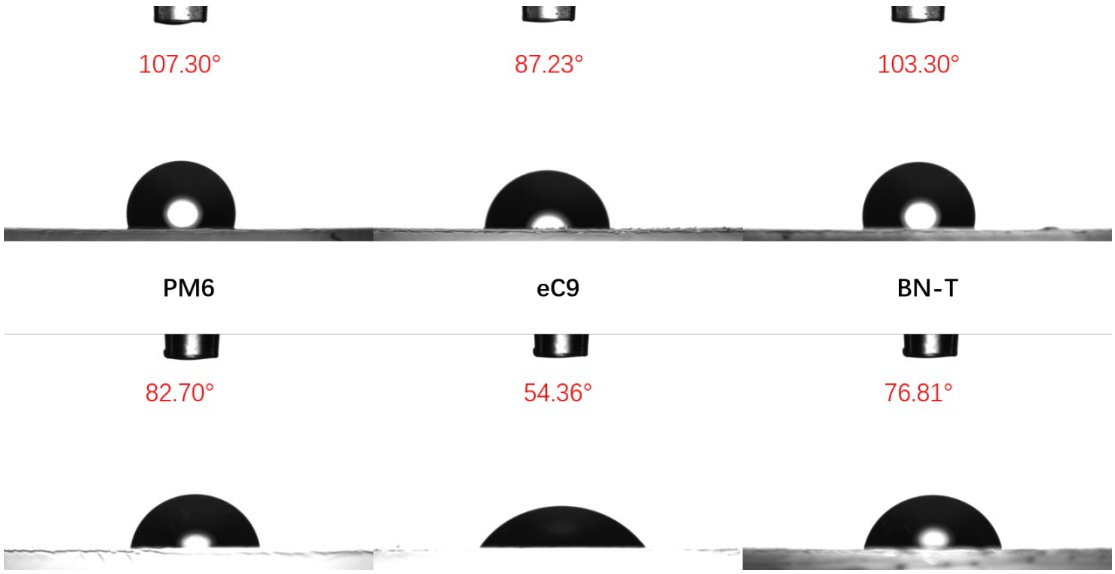

Figure S11. Contact angles of water (upper) and ethylene glycol (lower) on the films for PM6, BN-T, eC9 (CB+DIO).

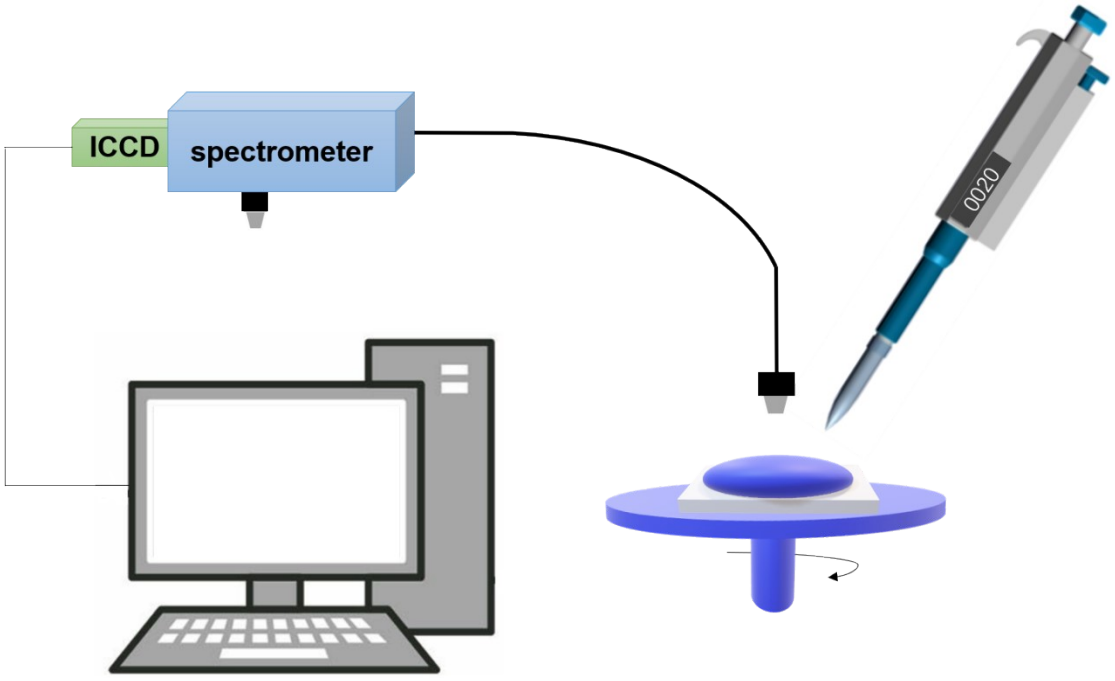

Figure S12. Operation pattern for data collection of film's real time reflectance.

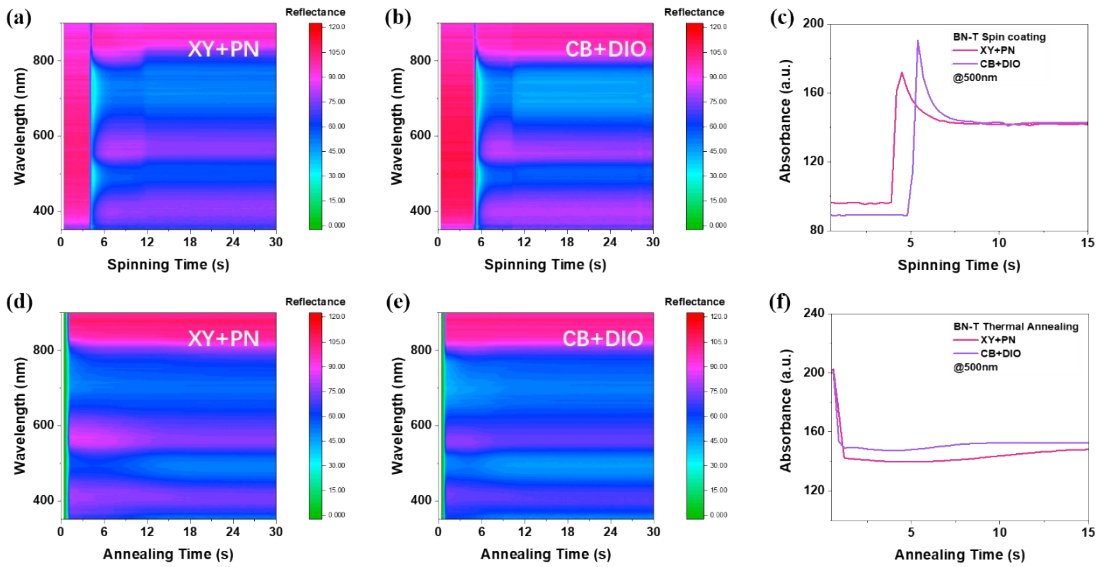

Figure S13. Contour maps of time & wavelength & reflection intensity of BN-T cast from cosolvents of XY+PN and CB+DIO, and correspondingly derived time resolved absorption at 720nm.

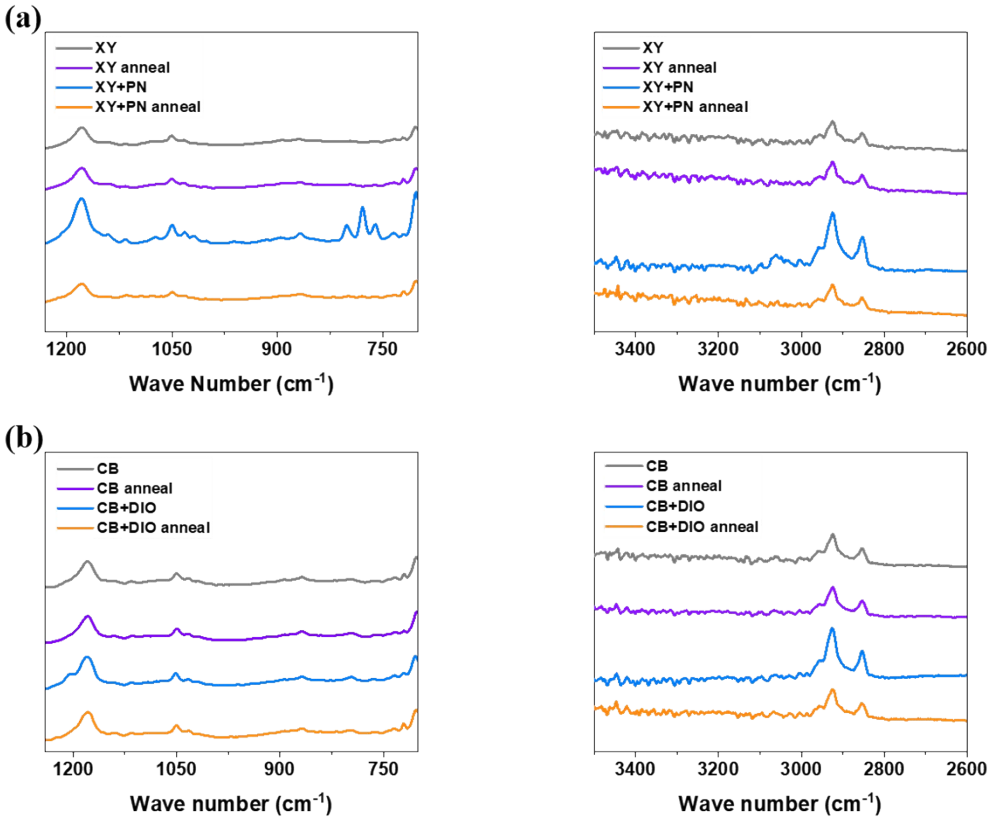

Figure S14. FT-IR spectra of BN-T's neat film cast by (a) XY+PN and (b) (CB+DIO) co-solvents, with or without thermal annealing.

Table S1. Photovoltaic performances of non-halogenated main solvent processed OSCs summary

Ref	Main Solvent(s)	Solvent additive(s)	V_{OC} (V)	J_{SC} (mA cm^{-2})	*FF* (%)	PCE (%)
Semi non-halogenated co-solvents						
1	Tol	DIO	0.86	26.33	0.77	17.43
2	XY	DIO	0.851	26.75	0.8	18.25
3	Tol	DIO	0.853	27.25	0.7814	18.16
4	Tol	DIO	0.879	26.7	0.809	19
5	Tol	CN	0.85	25.76	0.781	17.12
6	Tol	CN	0.933	22.52	0.738	15.51
7	Tol	CN	0.947	22.78	0.746	16.1
8	THF	DIO	0.85	25.2	0.75	16.1
9	Tol	DIO	0.84	26.9	0.796	18
10	XY	DIO	0.91	20.5	0.74	13.8
11	TMB	DIO	0.94	19	0.7	12.5
Single-component non-halogenated co-solvents						
12	TMB		0.865	26.05	0.77	17.36
13	XY		0.856	24.94	0.755	16.1
14	Tol		0.84	26.23	0.75	16.52
15	THF		0.96	17.97	0.7	12.1
16	Tol		0.95	18.19	0.7	12.22
17	anisole		1	18.9	0.63	11.9
18	MeTHF		0.92	22.47	0.667	13.8
19	MeTHF		0.88	17.62	0.76	11.76
Full non-halogenated co-solvents						
20	TMB	PN	0.784	19.8	0.73	11.7
21	Tol	BV	0.85	26.1	0.78	17.33
22	XY	1-MN	0.95	22.1	0.741	15.62
23	Tol	PN	0.88	24.3	0.726	15.6
24	THF	NMP	0.89	21.1	0.76	14.2
25	XY	PN	0.89	23.4	0.67	13.97
26	XY	PN	0.97	18.74	0.72	13.1
27	Tol	DPE	0.95	18.67	0.71	12.6
28	o-XY	NMP	0.83	19.2	0.74	11.83
29	XY	DPE	0.78	20.37	0.73	11.77
30	Tol	ODT	1.01	17.89	0.63	11.39
31	TMB	XY	0.82	28.15	0.778	18
32	XY	CS2	0.85	26.2	0.789	17.6
This work	**XY**	**PN**	**0.856**	**26.535**	**0.793**	**18.02**

Table S2. In-plane GIWAXS parameters of PM6:eC11:BN-T (XY+PN).

Ratio	Lamellar		
	Peak ($Å^{-1}$)	d-spacing (Å)	CCL (Å)
1:1.2:0	0.297	21.19	72.15
1:1.2:0.1	0.299	21.00	74.95
1:1.2:0.2	0.298	21.10	66.93

Table S3. Out-of-plane GIWAXS parameters of PM6:eC11:BN-T (XY+PN).

Ratio	Lamellar			π-π stacking		
	Peak ($Å^{-1}$)	d-spacing (Å)	CCL (Å)	Peak ($Å^{-1}$)	d-spacing (Å)	CCL (Å)
1:1.2:0	0.300	20.94	19.02	1.689;1.870	3.72;3.36	27.10;32.59
1:1.2:0.1	0.296	21.25	15.95	1.715;1.893	3.66;3.32	22.34;38.75
1:1.2:0.2	0.304	20.64	11.14	1.686;1.888	3.73;3.33	18.87;44.06

Table S4. In-plane GIWAXS parameters of PM6:eC9:BN-T (CB+DIO).

Ratio	Lamellar		
	Peak ($Å^{-1}$)	d-spacing (Å)	CCL (Å)
1:1.2:0	0.301	20.89	79.17
1:1.2:0.1	0.304	20.68	77.05
1:1.2:0.2	0.303	20.77	74.75

Table S5. Out-of-plane GIWAXS parameters of PM6:eC9:BN-T (CB+DIO).

Ratio	Lamellar			π-π stacking		
	Peak ($Å^{-1}$)	d-spacing (Å)	CCL (Å)	Peak ($Å^{-1}$)	d-spacing (Å)	CCL (Å)
1:1.2:0	0.325	19.33	64.74	1.792	3.51	21.77
1:1.2:0.1	0.325	19.35	72.84	1.824	3.45	23.60
1:1.2:0.2	0.320	19.62	84.09	1.812	3.47	22.56

Reference

1. D. Wang, H. Liu, Y. Li, G. Zhou, L. Zhan, H. Zhu, X. Lu, H. Chen and C.-Z. Li, *Joule*, 2021, **5**, 945-957.

2. D. Wang, G. Zhou, Y. Li, K. Yan, L. Zhan, H. Zhu, X. Lu, H. Chen and C.-Z. Li, *Adv. Funct. Mater.*, 2022, **32**, 2107827.

3. R. Sun, T. Wang, Y. Wu, M. Zhang, Y. Ma, Z. Xiao, G. Lu, L. Ding, Q. Zheng, C. J. Brabec, Y. Li and J. Min, *Adv. Funct. Mater.*, 2021, **31**, 2106846.

4. Y. Cui, Y. Xu, H. Yao, P. Bi, L. Hong, J. Zhang, Y. Zu, T. Zhang, J. Qin, J. Ren, Z. Chen, C. He, X. Hao, Z. Wei and J. Hou, *Adv. Mater.*, 2021, **33**, 2102420.

5. H. Chen, H. Lai, Z. Chen, Y. Zhu, H. Wang, L. Han, Y. Zhang and F. He, *Angew. Chem. Int. Ed.*, 2021, **60**, 3238-3246.

6. L. Jin, R. Ma, H. Liu, W. Xu, Z. Luo, T. Liu, W. Su, Y. Li, R. Lu, X. Lu, H. Yan, B. Z. Tang and T. Yang, *ACS Applied Materials & Interfaces*, 2021, **13**, 34301-34307.

7. S. Ding, R. Ma, T. Yang, G. Zhang, J. Yin, Z. Luo, K. Chen, Z. Miao, T. Liu, H. Yan and D. Xue, *ACS Applied Materials & Interfaces*, 2021, **13**, 51078-51085.

8. L. Hong, H. Yao, Z. Wu, Y. Cui, T. Zhang, Y. Xu, R. Yu, Q. Liao, B. Gao, K. Xian, H. Y. Woo, Z. Ge and J. Hou, *Adv. Mater.*, 2019, **31**, 1903441.

9. Y. Xu, Y. Cui, H. Yao, T. Zhang, J. Zhang, L. Ma, J. Wang, Z. Wei and J. Hou, *Adv. Mater.*, 2021, **33**, 2101090.

10. C.-Y. Liao, Y. Chen, C.-C. Lee, G. Wang, N.-W. Teng, C.-H. Lee, W.-L. Li, Y.-K. Chen, C.-H. Li, H.-L. Ho, P. H.-S. Tan, B. Wang, Y.-C. Huang, R. M. Young, M. R. Wasielewski, T. J. Marks, Y.-M. Chang and A. Facchetti, *Joule*, 2020, **4**, 189-206.

11. H. Guo, Y. Zhang, L. Chen, X. Liao, Q. Xie, Y. Cui, B. Huang, C. Yang and Y. Chen, *J. Mater. Chem. A*, 2019, **7**, 27394-27402.

12. R. Ma, T. Yang, Y. Xiao, T. Liu, G. Zhang, Z. Luo, G. Li, X. Lu, H. Yan and B. Tang, *ENERGY & ENVIRONMENTAL MATERIALS*, 2021, DOI: 10.1002/eem2.12226

13. S. Dong, T. Jia, K. Zhang, J. Jing and F. Huang, *Joule*, 2020, **4**, 2004-2016.

14. R. Sun, T. Wang, Z. Luo, Z. Hu, F. Huang, C. Yang and J. Min, *Solar RRL*, 2020, **4**, 2000156.

15. Y. Qin, L. Ye, S. Zhang, J. Zhu, B. Yang, H. Ade and J. Hou, *J. Mater. Chem. A*, 2018, **6**, 4324-4330.

16. Y. Xiong, L. Ye, A. Gadisa, Q. Zhang, J. J. Rech, W. You and H. Ade, *Adv. Funct. Mater.*, 2019, **29**, 1806262.

17. D. Liu, B. Yang, B. Jang, B. Xu, S. Zhang, C. He, H. Y. Woo and J. Hou, *Energy Environ. Sci.*, 2017, **10**, 546-551.

18. C. Zhu, Z. Li, W. Zhong, F. Peng, Z. Zeng, L. Ying, F. Huang and Y. Cao, *Chem. Commun.*, 2021, **57**, 935-938.

19. L. Zhu, M. Zhang, W. Zhong, S. Leng, G. Zhou, Y. Zou, X. Su, H. Ding, P. Gu, F. Liu and Y. Zhang, *Energy Environ. Sci.*, 2021, **14**, 4341-4357.

20. J. B. Zhao, Y. K. Li, G. F. Yang, K. Jiang, H. R. Lin, H. Ade, W. Ma and H. Yan, *Nat. Energy*, 2016, **1**, 15027.

21. X. Xu, L. Yu, H. Yan, R. Li and Q. Peng, *Energy Environ. Sci.*, 2020, **13**, 4381-4388.

22. B. Liu, H. Sun, J.-W. Lee, J. Yang, J. Wang, Y. Li, B. Li, M. Xu, Q. Liao, W. Zhang, D. Han, L. Niu, H. Meng, B. J. Kim and X. Guo, *Energy Environ. Sci.*, 2021, **14**, 4499-4507.

23. B. Du, Y. Ma, C. Guo, J. Cai, D. Li, S. Cheng, D. Liu, Q. Zheng and T. Wang, *Adv. Funct.*

Mater., 2021, **31**, 2105794.
24. Y. Cui, H. Yao, L. Hong, T. Zhang, Y. Xu, K. Xian, B. Gao, J. Qin, J. Zhang, Z. Wei and J. Hou, *Adv. Mater.*, 2019, **31**, 1808356.
25. S. J. Jeon, Y. W. Han and D. K. Moon, *Small*, 2019, **15**, 1902598.
26. W. Zhao, S. Zhang, Y. Zhang, S. Li, X. Liu, C. He, Z. Zheng and J. Hou, *Adv. Mater.*, 2018, **30**, 1704837.
27. X. Xu, T. Yu, Z. Bi, W. Ma, Y. Li and Q. Peng, *Adv. Mater.*, 2018, **30**, 1703973.
28. T. Kumari, S. Jung, Y. Cho, H.-P. Kim, J. W. Lee, J. Oh, J. Lee, S. M. Lee, M. Jeong, J. M. Baik, W. Jo and C. Yang, *Nano Energy*, 2020, **68**, 104327.
29. S. Rasool, Q. V. Hoang, D. Van Vu, T. T. Trang Bui, S.-M. Jin, T. T. Ho, C. E. Song, H. K. Lee, S. K. Lee, J.-C. Lee, S.-J. Moon, E. Lee and W. S. Shin, *J. Mater. Chem. A*, 2019, **7**, 24992-25002.
30. Y. Tang, H. Sun, Z. Wu, Y. Zhang, G. Zhang, M. Su, X. Zhou, X. Wu, W. Sun, X. Zhang, B. Liu, W. Chen, Q. Liao, H. Y. Woo and X. Guo, *Adv. Sci.*, 2019, **6**, 1901773.
31. B. Fan, F. Lin, J. Oh, H. Fu, W. Gao, Q. Fan, Z. Zhu, W. J. Li, N. Li, L. Ying, F. Huang, C. Yang and A. K. Y. Jen, *Adv. Energy Mater.*, 2021, **11**, 2101768.
32. X. Song, P. Sun, D. Sun, Y. Xu, Y. Liu and W. Zhu, *Nano Energy*, 2022, **91**, 106678.